A low-frequency buncher field-variation study on a 750 keV H- beam to increase Drift Tube Linac capture

Roy, Prabir Kumar
Taylor, Charles Edward
Pillai, Chandra

To be published in: Nuclear Instruments and Methods in Physics Research Section A: Accelerators, Spectrometers, Detectors and Associated Equipment

DOI to publisher's version: 10.1016/j.nima.2021.165464

Journal Pre-proof

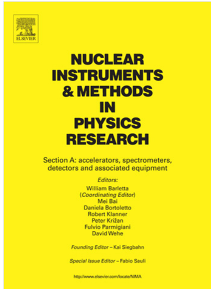

A low-frequency buncher field-variation study on a 750 keV H^{-} beam to increase Drift Tube Linac capture

Prabir K. Roy, Charles E. Taylor, Chandra Pillai

PII: S0168-9002(21)00449-6
DOI: https://doi.org/10.1016/j.nima.2021.165464
Reference: NIMA 165464

To appear in: *Nuclear Inst. and Methods in Physics Research, A*

Received date : 18 December 2020
Revised date : 10 May 2021
Accepted date : 15 May 2021

Please cite this article as: P.K. Roy, C.E. Taylor and C. Pillai, A low-frequency buncher field-variation study on a 750 keV H^{-} beam to increase Drift Tube Linac capture, *Nuclear Inst. and Methods in Physics Research, A* (2021), doi: https://doi.org/10.1016/j.nima.2021.165464.

A low-frequency buncher field-variation study on a 750 keV H⁻ beam to increase Drift Tube Linac capture

Prabir K. Roy,[1,*] Charles E. Taylor,[1] and Chandra Pillai[1]

[1] *AOT-AE, LANSCE, Los Alamos National Laboratory, Los Alamos, NM 87545, USA*

Abstract

Low-frequency (such as 16.77 MHz) RF bunchers are widely used in RF accelerator systems for longitudinal compression of pulses into a single RF bucket, which increases instantaneous beam intensity for time-dependent studies. In this study, the dependency of capture into a 201.25 MHz Drift Tube Linac (DTL) was measured as a function of gap voltage for a 16.77 MHz buncher on chopped H^- beam (approximately 25 ns at 750 keV, 10 mA peak current). The multiparticle code PARMILA was used to simulate the phase-space distribution of the 10 mA, 750 keV, H^- beam at the entrance to DTL with a wide range of the Low-Frequency Buncher (LFB) field (10 kV to 35 kV). The measurement and simulation indicated that the DTL capture could be dilute (reduced) for a non-optimized buncher field to a pre-configured beamline geometry. The data shows that changing the bunch field while keeping the incoming beam current and energy constant does not significantly alter the beam's emittance. However, downstream beam capture into the DTL is changed for a non-optimized phase-space bunching distance with the buncher field.

Usage: Beam bunch, Low-Frequency Buncher, Acceleration gap, RF cavity field measurement, emittance, radial electric field, RF Linac.

PACS numbers: 29.20.-c, 29.20.Ej, 29.27.-a, 41.75.Ak, 41.75.Cn.

I. INTRODUCTION

RF bunchers are optimized in charged particle beam accelerator systems to a specific design or experimental needs [1]. Some of these are (a) specialized compression of the beam particle distribution [2], (b) enhancement of current density, (c) beam pulse separation and minimization of bunch lengths [3], (d) longitudinal phase-space manipulation [4], (e) time-jitter study [5], and (f) beam loss study [6], etc. In the Los Alamos Neutron Science Center (LANSCE) accelerator system, an RF buncher is used with long wavelengths to bunch several H^- pulses into a single RF bucket for the 805 MHz acceleration frequency [7], and thus to enhance the peak-beam current in a micropulse. The phase-space bunching [8, 9] for micropulses is initially formed in the low energy (750 keV) beam transport (LEBT)

* pkroy@lanl.gov

section [10, 11]. A 16.77 MHz buncher, called the low-frequency buncher (LFB), is used to highly bunch the H^- beam for one (Weapon Neutron Research) of five user facilities. The LFB takes roughly four normal beam bunches' equivalence and compresses them into a single bunch less than 5 ns long. In general, the buncher parameters (voltage and phase) are optimized for the production beam. Yet, there is considerable interest in the stability of beam parameters with minor or significant LFB voltage changes to maintain capture. The capture is defined in percent by current measured (I_D) after entry to the DTL's design separatrix divided by the incoming beam current(I_b), i.e.,(I_D/I_b)100%. It could be easier to access capture study for any perturbation of the field and phase of a buncher, if there was any pre-existing documentation in house or in the literature. In a theoretical study [12], it was summarized that in RF cavities, emittance growth and halo generation in beams with smaller radii are small up to a certain space-charge current and increase linearly with the fourth power of the radius. But these studies do not discuss the effects a beam may experience if the RF cavity field was varied in the midway of a transport line. Thus, an experimental observation was necessary. The motivation of this work is to understand how varying the LFB field on a constant-current-beam affect in measurements (1) beam spot size, (2) beam capture, and (3) final beam quality. Better beam quality is defined as reduced beam current losses and reduced radiation spill [13] in the transport. The beam current loss is the loss of the charged particles from the primary beam. When a high energy loss particle strikes a drift tube wall or devices, it generates x-ray, gamma-ray, etc. – these are radiation spill. Transverse beam emittance and acceptance into the 201.25 MHz DTL were measured as a function of gap voltage to refine tuning of the 750 keV H^- beam. A phase-space distribution of the beam at the entrance to DTL was simulated using the multiparticle code PARMILA [14–17]. Experimental and PARMILA simulated beam sizes for variation of the LFB voltage were evaluated. The results of this study might be useful to beam operation. To have a better view of the study, the setup of the beamline and beam pulse time structure are described below.

II. BEAM TIME STRUCTURE

The LANSCE [18] linear accelerator utilizes H^+ and H^- [19] beams to support multiple experimental areas [18, 20]. The H^+ is used for the isotope production facility (IPF) [21],

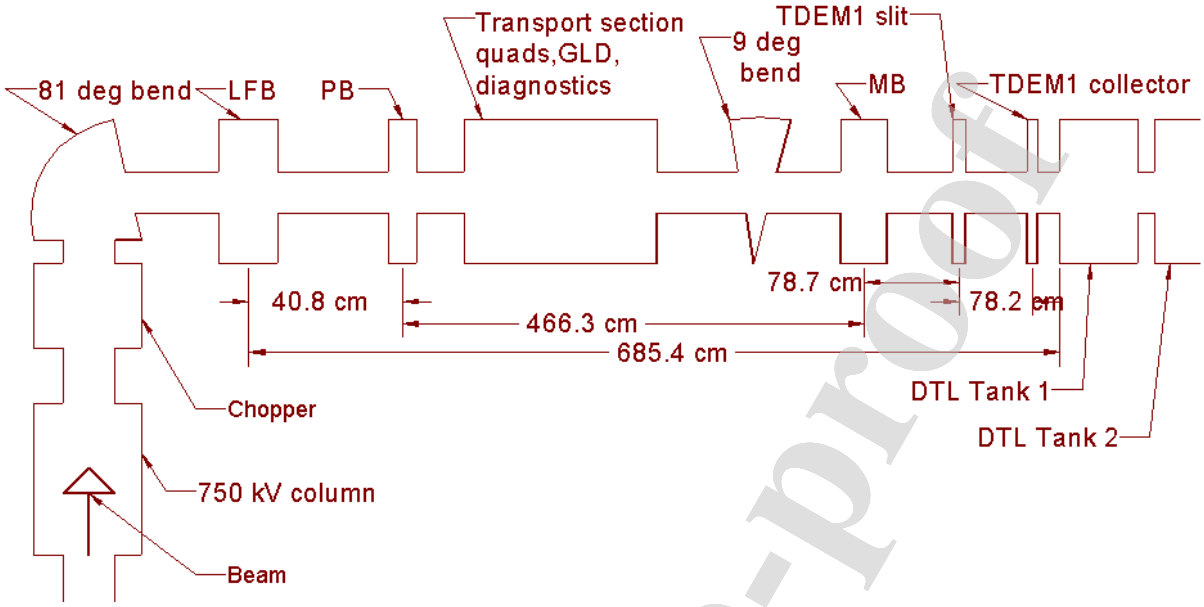

FIG. 1. A sketch of the major components of the 750 keV beamline, which consists of 16.77 MHz low-frequency buncher (LFB); 201.25 MHz Pre-Buncher (PB), 201.25 MHz Main Buncher (MB). Other components, such as quads, Bending Magnet (BM), Steering Magnet (SM), diagnostics, Ground Level Deflector (GLD), emittance scanner (TDEM1 slit, and collector) etc., are also located in the transport section. A current monitor (TDCM1) is situated between the TDEM1 slit and the collector. The choice of beamline length is based on other calculations in the past.

while the H^- species are used for the Weapon Neutron Research (WNR) [18, 22], Proton Radiography (pRad) [20] and Lujan Neutron Spallation Center. Cockcroft-Walton [23] based injectors are used to accelerate H^-, and H^+ beams up to 750 keV.

A schematic of the H^- LEBT section of the beamline is shown in Fig. 1. The pre-Buncher (PB) and Main Buncher (MB) operate at 201.25 MHz, which is the fundamental frequency of the LANSCE accelerator. These two bunchers are used with the right phases and amplitudes to bunch the 625 μs chopped beam into the 201.25 MHz DTL. The LFB is used to increase the charge per bunch, thus to increase the peak current for the WNR facility. The LFB increases the charge per microbunch ($\leq$5 ns) over what would result if only the 201 MHz pre-buncher and main buncher were used. In conjunction with the chopper, the LFB also aids in removing the sidelobes and satellite peaks (low amplitude signals) around the main single. The frequency (16.77 MHz) is selected by meeting several criteria: (1) it is a sub-harmonic of the 201.25 MHz to ensure it could be phase-locked to the 201.25 MHz

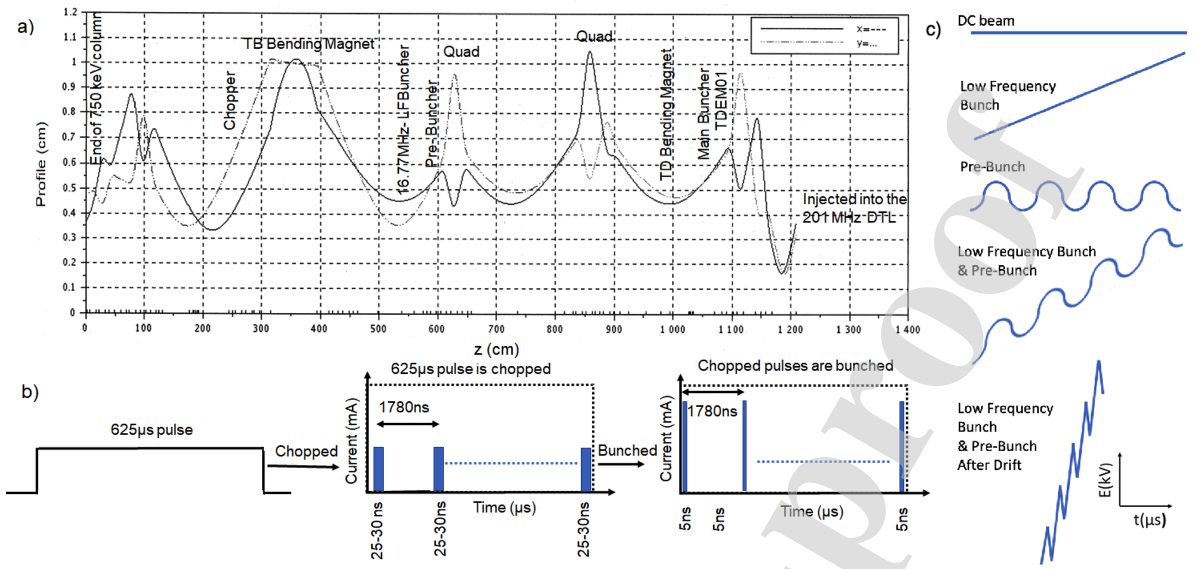

FIG. 2. (a) A typical 750 keV beam envelope section is starting from the end of the 750 keV column to the first Drift Tube Linac; (b) the temporal pulse length before chopping, chopped pulses, and the bunched beam of the chopped pulses; (c) longitudinal bunching of WNR beam, with LFB and pre-buncher modulation and the subsequent drift downstream.

reference (thus the integer 12=201.25/16.77), (2) it is low enough to allow sufficient charge to be bunched and captured into a 201.25 MHz RF bucket, 3) it could produce enough spacing between microbunches to allow the desired time-of-flight experiments at WNR to be performed without wrap-around problems; and 4) it could create a bunching structure that was a size that could be easily constructed, yet not so big that it would not fit in the transport, H^- transport line.

Figure 2(a) shows a typical beam envelope of a 10 mA (peak) H^- beam from the exit of the 750 kV column to the entry point of the DTL. Figure 2(b) shows a time structure of the beam. Figure 2(c) shows a process of longitudinal bunching for the WNR beam. The long-pulsed (625 μs) H^- beam is chopped for micropulses (25 ns - 30 ns) and is converted into bunches ($\leq$5 ns) and injected into the 201.25 MHz DTL cavities. After traversing all four DTL tanks, the bunch energy increases to 100 MeV. The H^+ species are deflected into the IPF line, while the H^- continues to the 805 MHz Coupled Cavity Linac (CCL). The final 800 MeV beam is then delivered to the Lujan, WNR, and pRad facilities.

As previously mentioned, the 625 μs direct current (DC) beam is chopped. Each of these chopped pulses is 36 ns wide. The pulse pattern width (PW) is typically set around 25-30 ns to account for the chopper's rise and fall time. The correct set point selection is determined by maximizing the charge per micropulse (typically spaced by 1780 ns, having a pulse width of 30 ns) without introducing charge into adjacent 201.25 RF buckets in the DTL. The exact number of spaced (τ) is defined as

$$\tau = \frac{CD}{f}, \tag{1}$$

where, CD is the countdown and f is the frequency of the LFB. So, if the CD = 30, then spacing is 1789 ns. The countdown is changeable as needed for the proton storage ring in the LANSCE facility. The low-frequency buncher acts on the chopped beam to concentrate it into a shorter pulse approximately 5 ns long. This short pulse is then injected into the 201.25 MHz main buncher and DTL systems, where it is further bunched and ultimately captured into a single RF bucket that produces the beam for WNR. By the end of the 800 MeV linac, the beam pulse width narrows to 100 ps. The LFB is only in-time with the WNR beam gate. The primary H^- pre-buncher was designed for beam to another experimental area but was found necessary for sufficient bunching of the WNR beam. The main buncher is primarily used to match the beam with DTL RF acceptance. Once the beam crosses the LFB, narrower bunching occurs across a distance as beam drifts downstream.

III. PHASE WIDTH BUNCHING DISTANCE AND THE BEAM TUNING

The performance of a buncher depends on the physical parameters of the buncher, such as the cavity length ($l = \beta\lambda/2$, β=particle velocity/light velocity, λ=light velocity/RF cavity frequency); field in the RF gap ($E_z(z,r,t) = E_g(z,r)cos(\omega t + \phi)$, where E_g is the max RF field, ω, t and ϕ are the angular frequency, time and synchronous phase, and z and r are the axial and radial components); incoming beam quality (beam size and halo, etc.).

The cavity RF field manipulates the phase space of the beam. The low-frequency buncher gap voltage sinusoidal modulates ($V_m = V_a \sin(\omega t)$, where V_m is the modulated voltage and V_a is the peak voltage) the beam energy. The cavity field applies a kick to the pulse. Due to rotation of the phase-space profile, a narrower bunch in phase is formed (phase-focused) at some drift distance (phase-focus distance), based on the correlation of time and off-momentum particle coordinates [24].

The minimum phase width bunching distance, L, from a cavity, is written as [7]

$$L = \frac{\lambda}{2\pi}\frac{mc^2(\beta_v)^3(\gamma_e)^3}{qV_0}, \quad (2)$$

where λ is the RF wavelength; m, c, q have their usual meaning of the mass, velocity of the light, and the charge of a particle; γ_e is the Lorentz energy factor; β_v is the relativistic velocity factor and V_0 is the peak voltage of cavity (a product of peak RF field and length of cavity).

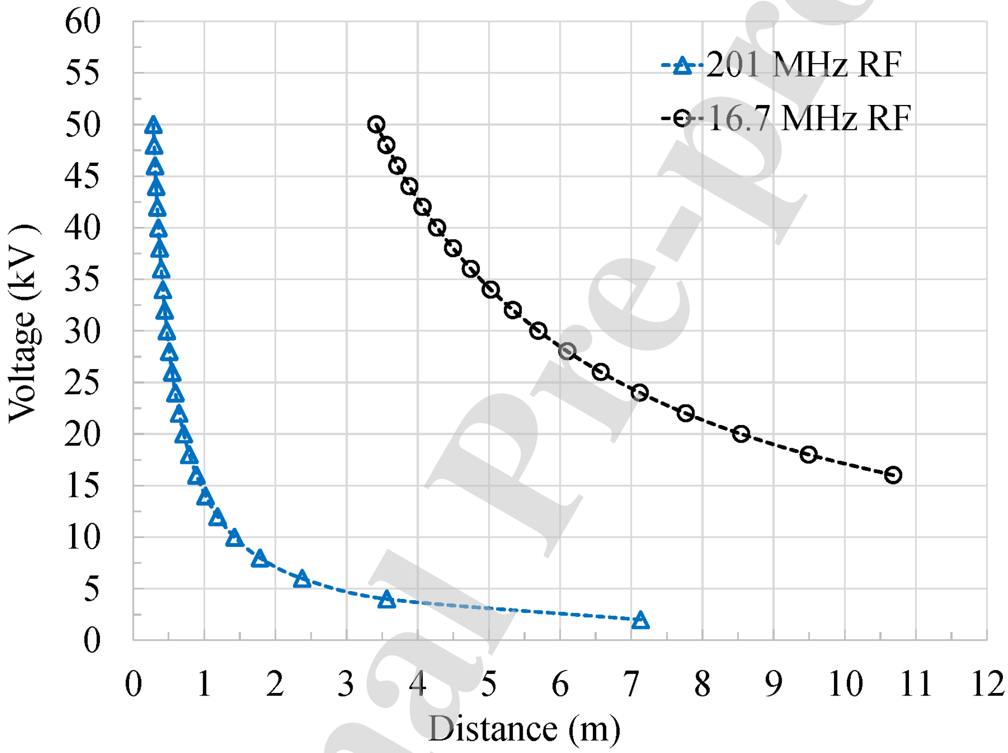

FIG. 3. A calculated result of bunching distance vs cavity peak voltage for 16.77 MHz (line with circles symbol) and 201.25 MHz RF frequency (line with the triangles), calculated using equation (2).

Figure 3 shows the minimum-phase-width bunching distance vs. peak voltage for frequencies of 16.77 MHz (line with circles), and 201.25 MHz (line with triangles), calculated using Eq. (2). The Lorentz energy factor (γ_e) =1+beam energy/proton rest energy, and relativistic velocity factor (β_v) are of 1.0008 and 0.04, respectively, for a H^- beam of energy 750 keV, used in this calculation. The graph shows that a bunch can occur both close to and far from the cavity as the magnitude of the peak voltage and frequency change. As a result, varying the LFB field can change the bunching location along the transport line.

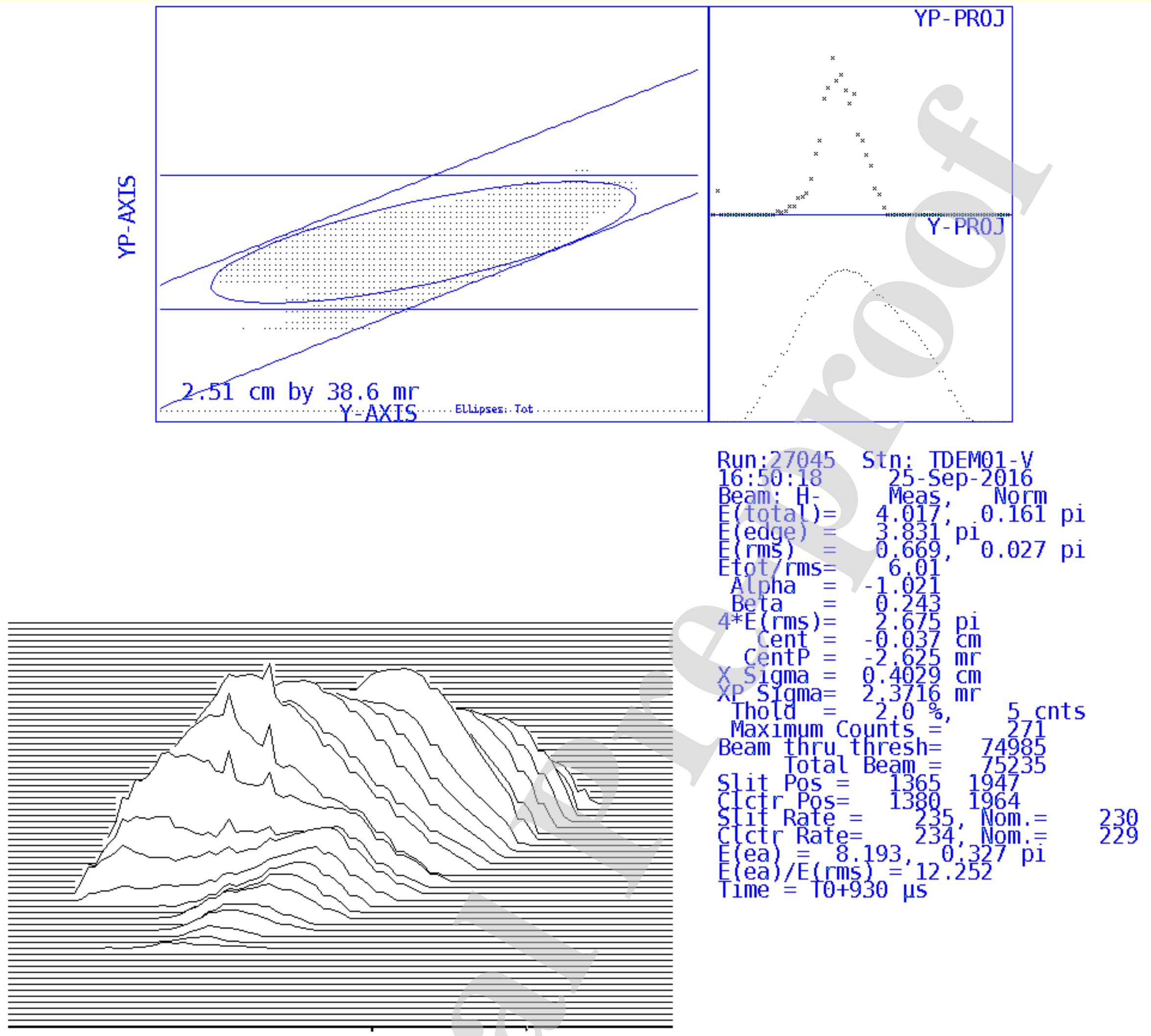

FIG. 4. An example of emittance measurement. A slit and collector based device (TDEM1) was used. Vertical scan emittance data are represented to the right side. The size and angle of the beam (here y and y′) of this measurement are shown in the top right.

The purpose of beam tuning (optimization) is to provide a matched beam with design Twiss parameters at critical transport points. The tuning method in this study was based on the data from emittance scan with its corresponding transport calculation [25]. Figure 4 shows an example of emittance measurement and data screen in this study. Data of the Twiss parameters, including emittance, are shown to the right side of Fig. 4 for a single measurement, as an example. A modified version of the 2D-TRACE [25] called SciTRACE code was used to obtain the beam envelope (Fig. 2a). The program inputs are α, β, and emittance (measurement as shown in Fig. 4). For the linear approximation, emittance,

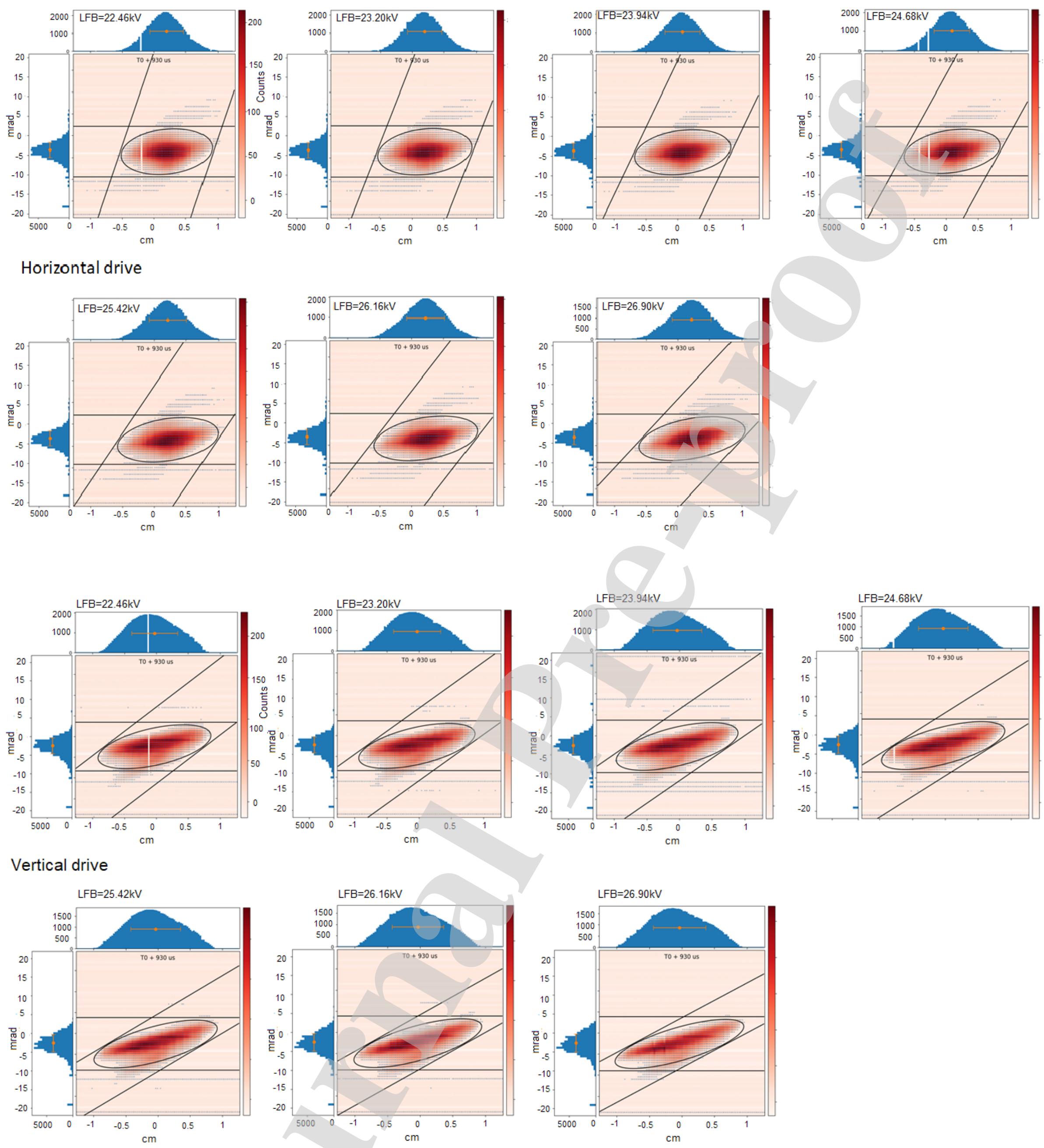

FIG. 5. Top two rows: x-x′, and emittance data for horizontal measurement; and bottom two rows: y-y′, and emittance data for vertical measurement, with the variation of the LFB voltage.

ε [26], in the (x, x′) -plane is related to the Courant-Snyder or Twiss parameters β, α and γ by $x = \sqrt{\beta\varepsilon}$ and $x' = \sqrt{\gamma\varepsilon}$, where $\gamma = \frac{1+\alpha^2}{\beta}$. If the dimensionless measure $\alpha > 0$, the beam converges. For $\alpha < 0$, the beam diverges; and $\alpha = 0$, the beam has minimum (waist) or maximum (peak) distribution. Twiss parameters are determined at particular locations by varying the magnets setpoints. Finally, TRACE is used to match the beam into the first tank of DTL based on the final emittance measurements. There are several points where it is particularly important to focus the beam (create a waist). These waists exist in the middle of a chopper [10], entrance to the pre-buncher (PB), middle of the ground level deflector (GDL), and entrance to the Main-Buncher (MB). In a good transport condition, initial Twiss parameters of the 80 keV, 10 mA beam, at the entry of 750 kV column, are roughly α_x=-0.270, β_x= 0.408 cm/mrad and 4*RMS un-normalized emittance, ϵ_x=6.11 π cm-mrad for the x-direction. The corresponding values for the y-direction are: α_y=-0.339, β_y= 0.436 cm/mrad, and 4*RMS un-normalized emittance, ϵ_y=5.66 π cm-mrad. The 2RMS beam size in the x and y directions are R_x=1.58 cm and R_y=1.57 cm, respectively. These numbers are altered based on how correctly the Pierce electrode is centered with the source converter during the source re-cycle time. Typically, these parameters are used in the TRACE to model the transport line in the 750 kV column. Then, further emittance is measured downstream at several locations to reach the desire Twiss parameters.

It is necessary to have a specific beam size at the first DTL tank entrance for ideal acceleration. For the 750 keV beam, typically, β_x= 0.026 cm/mrad in the x-plane, and β_y= 0.0059 cm/mrad in the y-plane are used, with a 4*RMS un-normalized emittance of 1.9 π cm-mrad to load the beam in the DTL. These translate to a 2RMS beam size with R_x=0.22 cm and R_y=0.106 cm, roughly, at the entrance of the first DTL. The minimum aperture size in the LFB setup is 1.90 cm (0.75 inches); an expected beam size to the aperture in the buncher is 0.45 cm (2RMS). Experimentally, the beam size at the aperture location is approximately 0.5 cm to 0.55 cm (2RMS), year to year. Thus the beam in general is 4 times smaller than the LFB aperture. The beam tuning [27], based on hardware and software [25] utilization, is performed to satisfy these requirements. Figure 5 shows measured x-x′ (for horizontal drive), y-y′ (for vertical drive), and emittance profiles for a variation of the LFB voltage from 22 kV to 26 kV, measured using TDEM1.

IV. BEAM PROFILE AND PHASE-SPACE ANALYSIS USING PARMILA

The computational program PARMILA was used to assess the beam particle distribution at the first DTL entrance. All necessary parameters for the focusing magnets, bending

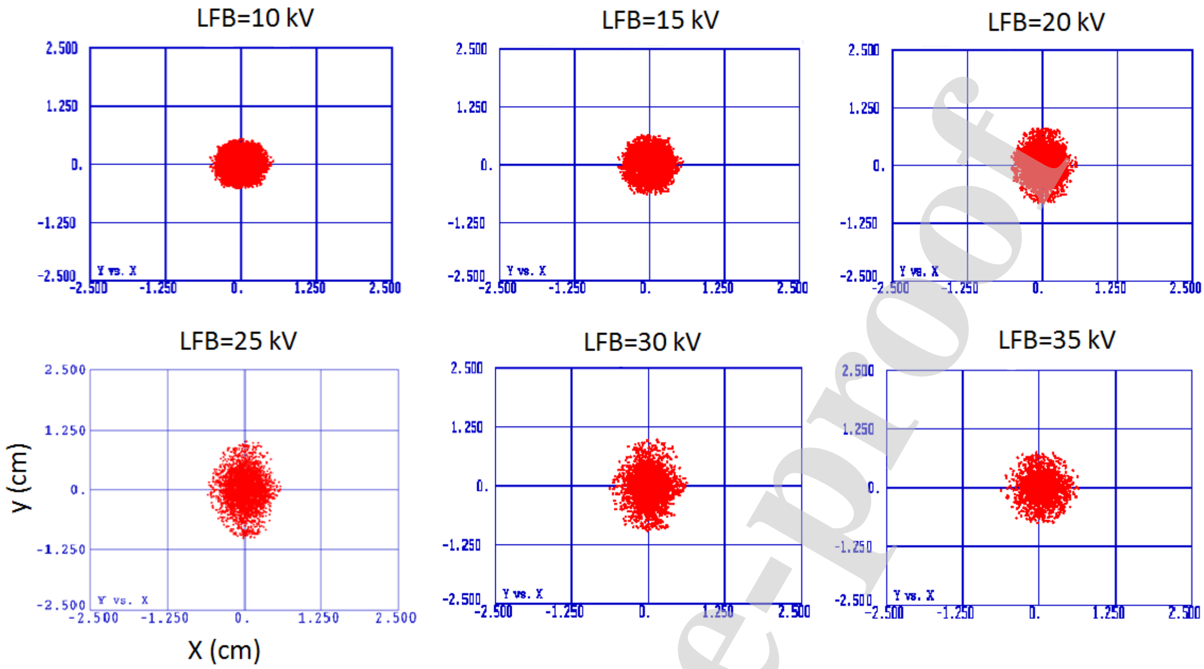

FIG. 6. The transverse beam distribution at the beam entry location of the first DTL tank, with the variation of LFB peak voltage, calculated using the PARMILA code. The low-frequency buncher (LFB) peak voltage was 10 kV, 15 kV, 20 kV, 25 kV, 30 kV, and 35 kV for a beam of 10 mA with 750 keV energy.

magnets, diagnostics, and drift lengths, beam parameters (starting energy=0.75 MeV, beam current=10 mA, the rest energy, mc^2= 939.30 MeV, charge number=1, and 0 degree phase shift) were taken into account in the code, starting at a distance from downstream of the chopper with 1.5 cm bore and ending up to upstream of the first DTL tank. The buncher radial aperture was set to 2.33 cm, the maximum energy gain to 0.025 MeV for a singly-charged particle at the crest of the RF field, cavity frequency to 16.77 MHz, and phase of -90^0 for the cavity RF field when synchronous or design particle is at the center of gap [17]. In PARMILA, a space-charge calculation is not performed for a cavity element. The pre-buncher cavity (201.25 MHz) power was set to 0, and the main buncher cavity (201.25 MHz) was powered with a maximum energy gain of 0.012 MeV (the main buncher voltage 12 kV was in this simulation). The maximum energy gain was calculated by [17];

$$\Delta W_{max} = qE_0 T l_{cav} \cos(\phi) = qTV \cos(\phi), \tag{3}$$

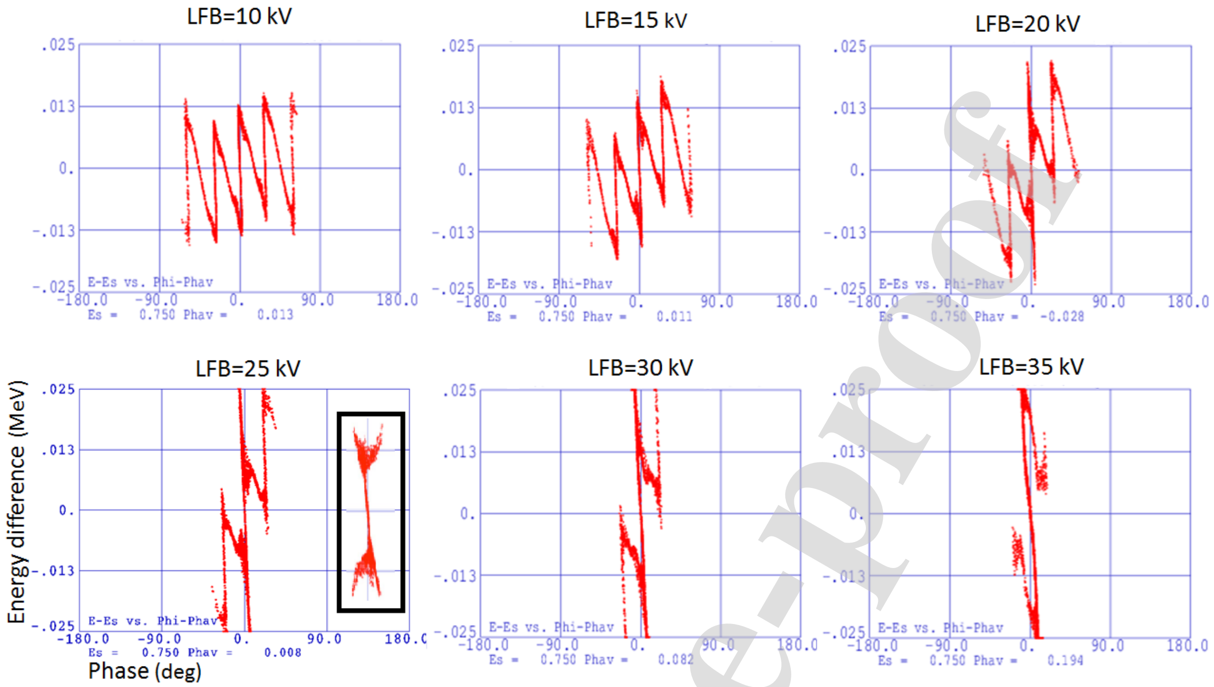

FIG. 7. The beam longitudinal phase space at the beam entry location of the first DTL tank, for a change of LFB peak voltage (calculated using PARMILA). The horizontal axis shows a phase of the beam in degrees and the vertical axis shows energy variation of the given energy. Simulated longitudinal phase space of the WNR beam at DTL [11] (201.25 MHz) is shown on the right side of the figure with LFB=25 kV.

where q is the particle charge, E_0 is the average axial electric field, T is the transit-time factor for velocity β_v of the design particle, and l_{cav} is the length over which E_0 has been defined, and ϕ is the synchronous phase. A calculated transit time factor of roughly 1 for an acceleration gap of 0.95 cm was utilized to study the energy gain.

Figure 6 shows the transverse beam distribution upstream (at the entrance) of the DTL with a variation of the LFB field. The spot size was mostly like round when the cavity was energized with a peak voltage of 10 to 15 kV. This shape was elongated (elliptical) transversely with the LFB voltage increase within a range of 20 to 30 kV. With a peak voltage of 35 kV, the beam spot size returned to a round form with scattered particles surrounding. The beam spot size in the y-direction is larger than the x-direction with the LFB voltage of 20 to 30 kV. The phase-space was rotated during the RF bunching by the buncher field. The coordinates of particles were rotated in phase space after the drift to bunch phase focus. Therefore, elongation of the beam with LFB voltage of 20 to 30 kV was due to bunching by the LFB voltage. Note that the main buncher voltage was not altered during the process.

Figure 7 represents the WNR micropulse beam phase-space distribution at the entrance to the DTL. The beam energy and phase spread were more significant, relatively, when the LFB was operated with a peak voltage higher than 10 kV to 15 kV (most notably at 25 kV). There were fine structures evident with a period of approximately 30° in Fig. 7. The main buncher most likely caused these structures. The signature of 30° was present since the LFB voltage varied from 10 kV up to 35 kV. We deliver the beam H^+ and H^- using the same transport line near the DTL (local name transport line TD). A single main buncher is used for both beam species, though these species come from two different beamlines (local name transport Line TA and Line TB). The H^+ beam is for isotope production, and H^- beam is used for WNR and other user facilities. The H^- beam was used in this study, but it was necessary to keep the main buncher on to keep the H^+ beam operational without interruption in production.

Figure 8 shows the beam particle accumulation in a bucket with a variation of LFB gap voltage. The beam particles were not accumulated well in a single bucket with 10 to 20 kV. The graph demonstrates the peak particle counts were relatively lower (as for an example, 370 vs. 530 arbitrary units) with a lower voltage. The phase spread was shrunk with a higher voltage.

In the simulation, a wide range of LFB field (10 kV to 35 kV) was used to observe a variety of phase-space distributions. In practice, there were limitations to using such a wide scale of the LFB field. In the experiment, the LFB field was narrowed down from 22 kV to 26 kV to maintain the RF system and hold the beam current on the collector up to the end of the 100 MeV DTL section.

V. EXPERIMENTAL MEASUREMENTS

The calibration of the 16.77 MHz cavity peak voltage is represented in Appendix A. The beam emittance was measured downstream of the bunchers (TDEM1 slit location). The position of the emittance slit was roughly a meter upstream of the first DTL tank. The beam size was measured [28] using a harp-type assembly, located just upstream of the

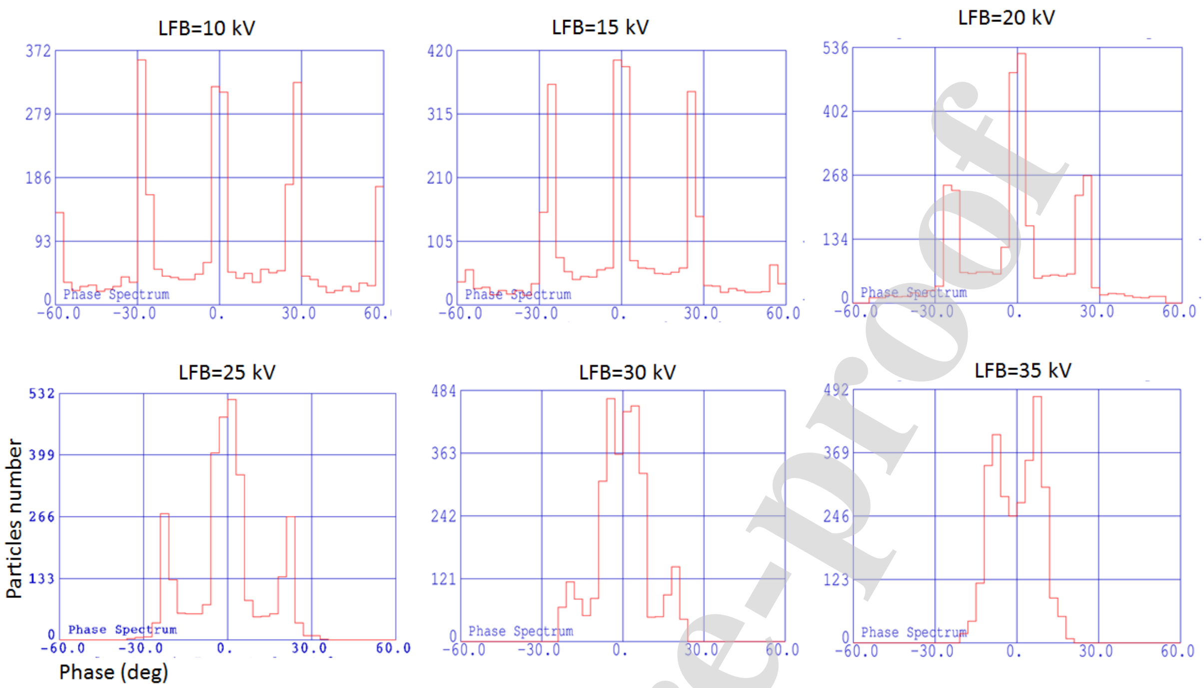

FIG. 8. The Phase spectrums for variation of a low-frequency (16.77 MHz) buncher voltage at the beam entry location of the first DTL tank. The graph shows the beam particles were not accumulated in a single bucket with a voltage of 10 to 25 kV but distributed to the slide lobes. When a higher voltage (30 kV) was utilized, the beam particles were accumulated in a single bucket, phase spread was shrunk, and the number of the particles was increased for consisting of a single bucket rather than spreading in phase.

emittance device. Harps are used to characterizing the beam profile of particle beams at LANSCE. The harp design at LANSCE's facility has a 7.6 cm profile width and 1 mm wire resolution. The harp head assembly needs 77 wires in both the horizontal and vertical planes. The beam current was measured between the slit and collector of the emittance station (TDEM1) and at the downstream end of tank 2 & 3 of the DTL. Figure 5 shows measured x-x′, y-y′, and emittance data, mentioned early. Table I shows measured x-x′, y-y′, emittance, and the beam current data. The horizontal (x) and vertical (y) sizes of the beam were increased likely 20% and 9%, respectively, with the LFB voltage variation of roughly 22 kV to 26 kV. A change of the modulated voltage (V_m) as well as the LFB field perturbed (over-read) the phase-focal distance of the beam (see Fig. 3).

Figures 9(a) and 9(b) show the Twiss parameters (α, β) with variation of the LFB gap

TABLE I. Data of measured beam-spot size using harp, beam current, and emittance with a variation of the low-frequency (16.77 MHz) buncher voltage. The emittance was measured using emittance-station TDEM1 (see Fig.1). The upstream current was measured using a current transformer located between the slit and collector of the TDEM1. The beam size was measured using a harp device at upstream (within several cm) of the TDEM1 slit. The downstream current was measured at downstream of the 2nd DTL.

LFB	**Size (16%-84%)**		**Angle (mr)**		**4*E(rms) (πcm-mrad)**		**Peak current (μA)**	
(kV)	**Hori.(x) (cm)**	**Ver.(y) cm**	**x'**	**y'**	**Hori.**	**Ver.**	**Upstream**	**Downstream**
22.46	0.56	0.84	3.87	4.31	2.02	2.67	442	247
23.20	0.59	0.85	3.88	4.35	2.05	2.66	449	241
23.94	0.62	0.87	3.76	4.52	2.02	2.75	444	215
25.42	0.64	0.88	3.74	4.60	2.07	2.70	449	200
26.16	0.65	0.90	3.72	4.68	2.08	2.72	441	183
26.90	0.67	0.91	3.7	4.74	2.09	2.68	441	162

voltage, measured using TDEM1. The experiment shows a decrease in α along with an increase in β with increase of LFB voltage. A small increase of 4*emittance (RMS) of 3.4% was observed, shown in Fig. 9(d), for a rise in LFB peak voltage (V_a) from 22.46 kV to 26.9 kV. The change however was within the uncertainty of measurement and was likely not significant.

Measured data of the beam size and Twiss parameters indicated that the beam was divergent, though the emittance was not altered significantly. A phase focus occurred in an earlier distance (see Fig. 3) with a higher voltage and afterwards was propagated with a modified envelope. A quadrupole magnet (local name TDQL1) was present in the transport section upstream of the collector (TDEM1). The strength of the magnet was un-altered during the LFB voltage variation study. However, the strength of the TDQL1 was powered zero during emittance measurement only to eliminate influence on the measurement. In the experiment, the beam envelope was not tuned further for each step change of the LFB voltage.

Figure 10 shows the beam size measurements were compared directly with PARMILA simulation. The regions of overlap show reasonable agreement. The measured data indicated

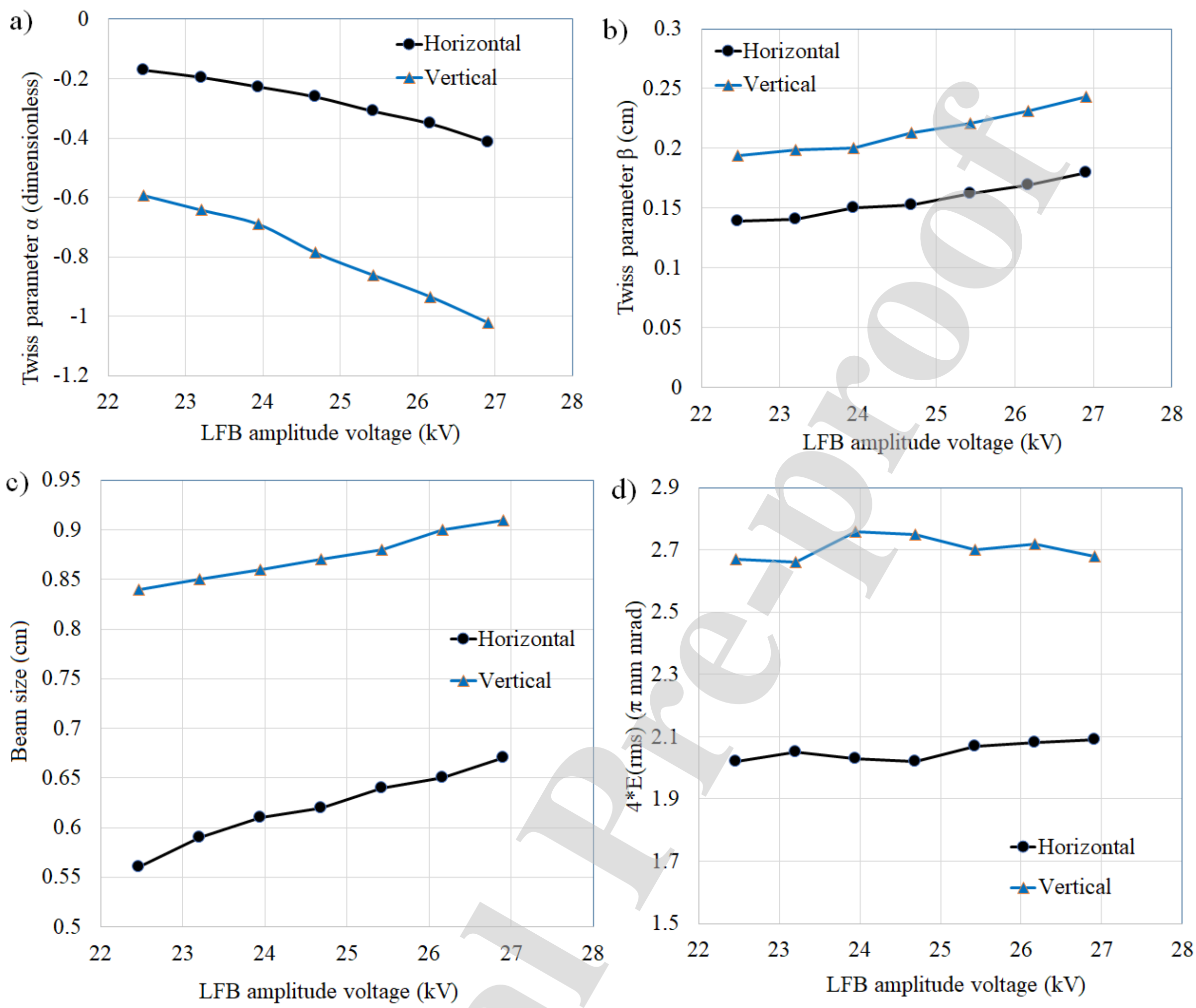

FIG. 9. (a) Measured values of the Twiss parameter α for horizontal and vertical scans of the emittance station TDEM1, with the variation of LFB amplitude setpoint; (b) Measured values of the Twiss parameter β, for horizontal and vertical scans, with the variation of 16.77 MHz LFB amplitude setpoint; (c) Measured beam size (2RMS) for horizontal and vertical coordinates at the slit location; and (d) Data of un-normalized emittance measurements using TDEM1. $4\times$ emittance (RMS) was changed by 3.4% with LFB amplitude set point variation from 22.46 kV to 26.90 kV.

that 24 kV to 26 kV are well matched with simulation. A transverse component of the cavity electric fields ($E_r = -\frac{r}{2}\frac{\partial E_z}{\partial z}$) are effected only if the experimental beam optics were off-axis. Yet, the possibility of the beam offset was negligible as it was tuned based on the optimization of the centroid.

Figure 11 shows measured current of the beam at 750 keV upstream (between TDEM1

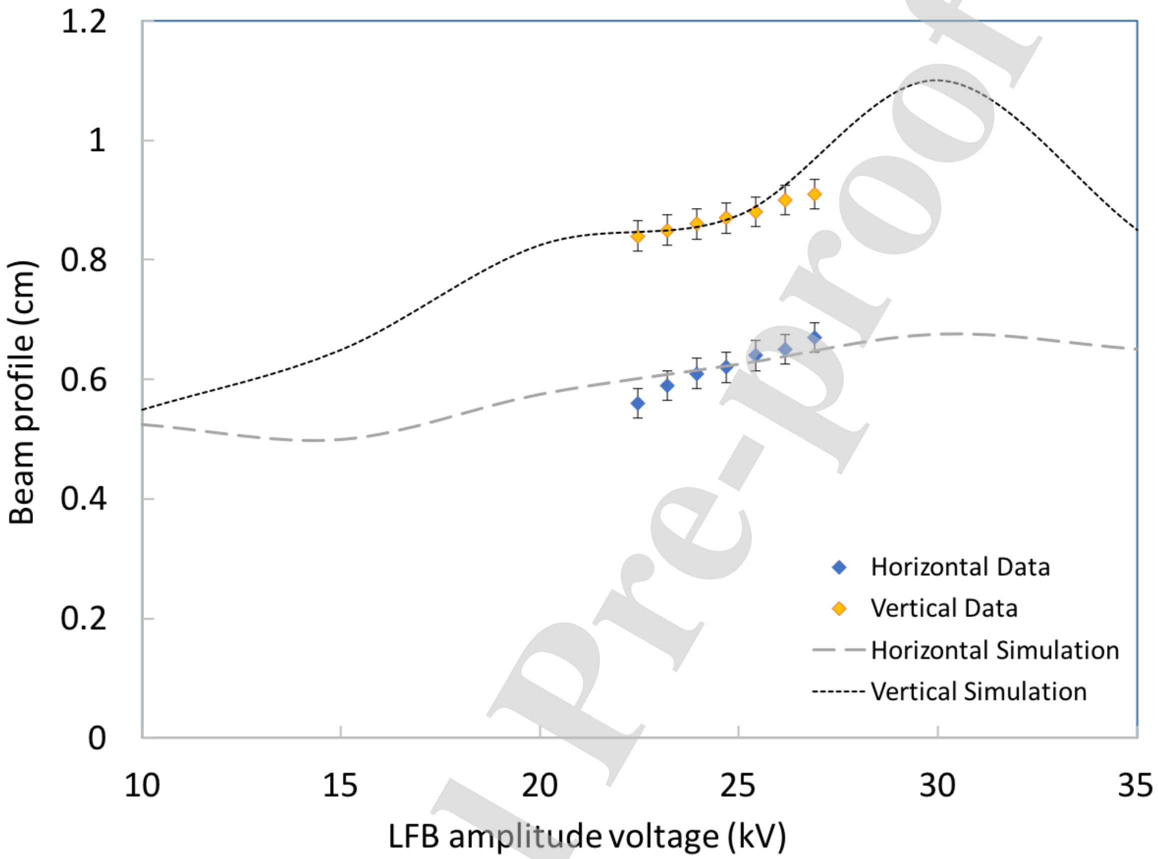

FIG. 10. Shows the measured change in the beam size (2RMS) for LFB variation, with a comparison to the simulated PARMILA response. The measurement uncertainty of the harp scan diagnostics is typically expected at a quarter of a millimeter.

slit and collector) of DTL, downstream of the second tank of DTL at 40 MeV, and the third tank of DTL (energy 72.7 MeV) with a change of LFB voltage. The peak beam current was the same ($\simeq 441\mu$A) at the lower energy side, for a change of 22.46 kV to 26.9 kV. The beam current of $\simeq$ 250 μA was measured downstream of tank 2 and tank 3 of DTL for 22.46 kV, but the current was changed to $\simeq$ 155 μA for 26.9 kV. These were due to loss of particle such as for divergence of the beam distribution and mismatch of the distribution with the aperture of the DTL (transverse and longitudinal mithmatch). In an-early-simulation [29] for the WNR, observed capture was likely 50% and simulated result was 45% with the

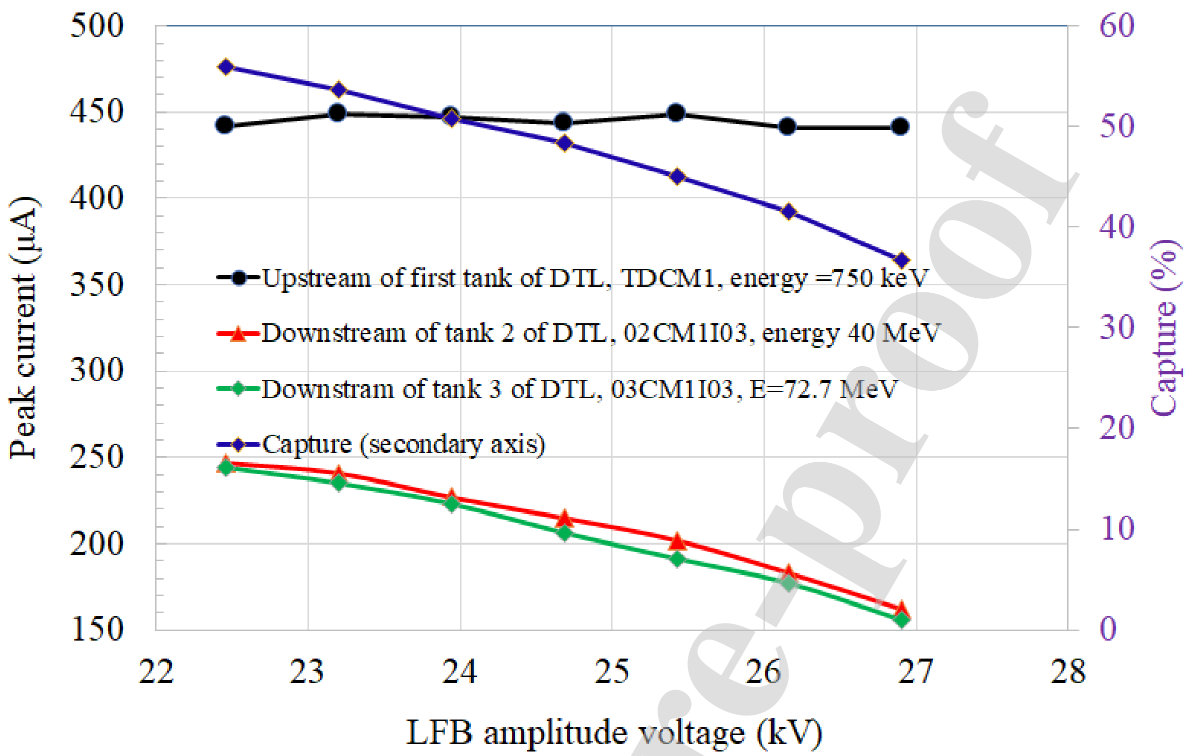

FIG. 11. Plot of the beam current (primary vertical axis) at 750 keV (between TDEM1 slit and collector), 40 MeV (downstream of the 2nd DTL), and 73 MeV (downstream of the 3rd DTL). The current captured into DTL was reduced (secondary vertical axis) with the increase of the LFB amplitude.

LFB=32 kV. In the simulation process, a model for the present WNR beam incorporating transverse and longitudinal beam dynamics through end of the DTL Tank 2 was created and then included debuncher in LEBT (Low Energy Beam Transport) section. The PARMILA was used to model the evolution of beam (multiparticle simulation required to represent an evolution of beam from unbunched to bunched). The modeling space was started at the end of 80 kV column and tracked particles to the end of DTL Tank 2 (included components vital to determining chopping, bunching, and capture of the beam). In the simulation, nominal transverse focusing strengths corresponding to a LANSCE production reasonable estimates for buncher fields were used. The simulation DTL design field, and experimental estimates of transverse beam emittance (IBEM at 80 keV), and best estimates for space charge compensation were also used. In simulation capture was calculated by DTL tank 2 beam current data / Beam current data measured at TDCM1 station. In a production beam, typically, the capture of the beam was higher as 80% for so called Long Bunch Enabled Gate (LBEG). The H^- Low Energy Beam Transport (LEBT) is tuned for the highly space-charge compensated LANSCE Lujan center beam (LEBG), which typically has a capture (02CM01/TDCM01) of about 75% to 80% for a 10 mA to 12 mA peak current. The capture is dominated by the beam's longitudinal properties, created by the prebuncher and main buncher, and the longitudinal acceptance of the DTL. Of the two bunchers, the main buncher has the most considerable effect on the capture. The situation is very different for the WNR (MPEG) beam that we present in this article. MPEG stands for Micro Pulse Enable Gate, which is the Master Timer beam gate designation for the nominal WNR micropulse beam. Instead of a sequence of adjacent micro- bunches separated by 5 ns, the WNR beam is a single micropulse space roughly 1.8 μs apart. To create this type of micropulse, the chopper is set to allow a 25-30 ns long slice of charge through. This slug of charge is bunched by the 16.77 MHz Low-frequency buncher instead of the pre-buncher. The LFB is the largest and most significant buncher for MPEG. Unlike the LBEG beam, the MPEG has little to no space-charge compensation, which means the beam is trying to blow itself apart once it leaves the chopper. As this slug of charge drifts to the main buncher, the energy modulation impressed on it by the LFB causes it to slowly bunch. The main buncher puts more phase-energy distortion on the microbunch leading to lower capture. One assumption is that the main reasons for the lower capture for MPEG have to do with the higher charge-per-pulse, the lower space-charge compensation and that the LFB is good but not great at doing the job it is asked to do. For a given beam development time, the beam's capture into the DTL was >55% for LFB peak voltage of 22.46 kV. This value was reduced to 37% at the DTL aperture, when the LFB cavity peak voltage increased. A significant loss of the beam current was not observed upstream of the first DTL tank with the increase of LFB voltage. It was inferred that the beam current monitor captured all the beam particles, even those that diverged, but was diluted gradually downstream for divergence. The beam's capture was significantly reduced with the increase of the LFB voltage near the optimal phase focus condition. As the emittance data was not changed dramatically, the capture was not diluted for the emittance. The Proton waveform can be observed on the wall current monitor in the WNR facility to aid in optimizing the longitudinal bunch form and transverse beam size.

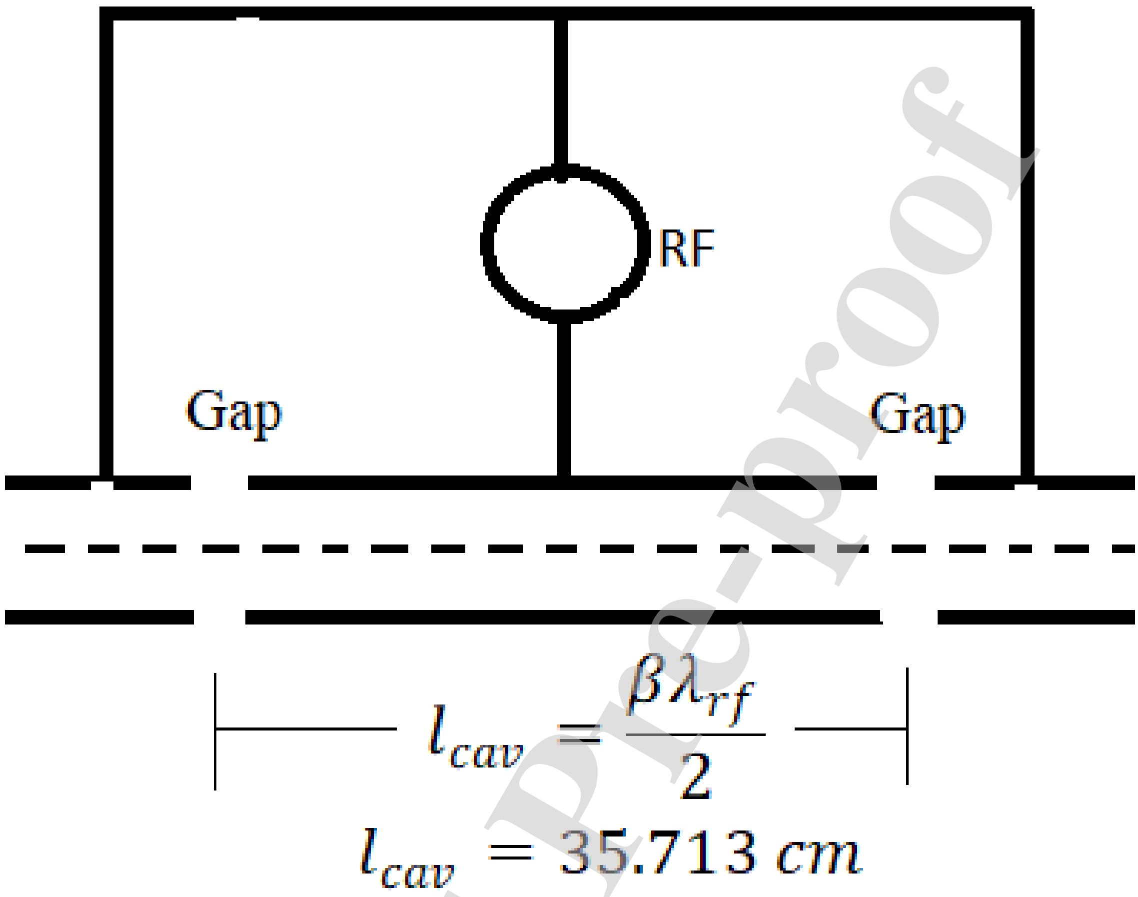

FIG. 12. The buncher consists of two gaps, each of 0.953 cm, separated by a distance of 35.7 cm. Synchronous particles travel this distance during 180° of RF rotation.

VI. CONCLUSION

A 16.77 MHz RF buncher called the low-frequency buncher (LFB) is used in conjunction with two fundamental frequency (201.25 MHz) bunchers (pre-buncher and main buncher) to increase the peak charge per pulse by a factor of three for the WNR experimental areas at LANSCE. Transverse beam emittance and capture into the 201.25 MHz Drift Tube Linac (DTL) were measured as a function of the LFB gap voltage. The multi-particle code PARMILA was used to simulate the beam's phase-space distribution at the entrance to DTL. Changes were observed downstream in the beam spot size, current, and Twiss parameters, increasing the LFB peak voltage. Data demonstrate that beam emittance was not altered significantly for the buncher field variation (Fig. 9d), but the beam divergence pattern was observed (Fig. 9a-c). Using PARMILA, it was observed that a round beam spot size could be vertically increased with an increase of the LFB voltage (Fig. 6) for phase-space rotation. In the experiment, as the LFB voltage was changed, the beam divergence occurred (Fig. 9). The capture changed dramatically (Fig. 11, right vertical axis) for the beam divergence (Fig. 9a-c). If the beam was not offset significantly, the effect of the radial electric field would be negligible. But any off-axis particle could receive a different kick of electromagnetic force at the gap and dilute emittance. But emittance dilution was not observed. The measurement and simulated results indicated that an optimal buncher field is required for a given geometrical configuration (length) of the beamline and the transport line elements (quadrupole). The space-charge effect was not included in this study. Though in another experiment [30], it was shown that a well-bunched beam could present an enhanced current in the pulse, and space charge was dominant that extended the beam spot size, energy variation can also dilute the beam spot size. In this study, compression ratio is very negligible compared to the literature [30]. Thus the space-charge effect is not considerable. However, Eq. 2, which is related to the beam energy, cavity voltage, and the operating frequency, demonstrates that phase focal location of the beam bunching is a crucial parameter to increase the DTL capture.

VII. ACKNOWLEDGMENTS

This work is supported by the Department of Energy, Division of High Energy and Nuclear Physics, under contract DE-AC52-06NA25396.

The authors are grateful to Larry Rybarcyk for many valuable suggestions and comments. The authors are grateful to Mark Gully and Nathan Moody for operational insight. Thanks to John Lyles, Janardan Upyadhaya, and En-Chuan Huang for contributing to measure LFB voltage, cavity field analysis and emittance analysis tool, respectively. LANL report number: LA-UR-20-25096.

Appendix A: Calibration of low-frequency buncher

Figure 12 shows a sketch of the two-gap cavity low-frequency buncher. The distance between the gap cavity is $\simeq$ 35.71 cm, known as cavity length. An acceleration gap length is 0.953 cm. The velocity of 750 keV low energy beam is 1.19x10^7 m/s; flight time through an acceleration gap is of $\leq$ 0.80 nsec. The operating frequency of the buncher is 16.77 MHz (60 nsec period). This frequency is 12 times smaller than the LANSCE DTL operating frequency. The main buncher of frequency 201.25 MHz modulates beam with the DTL 201.25 MHz frequency.

The cavity setpoint was calibrated [31] using a known method [32, 33] that measures RF voltage by correlation of RF and DC voltage breakdown between a pair of carefully spaced spherical electrodes. It was observed that the voltage breakdown threshold is lower by several kV RF signals than the DC level. As an example, a 15 kV DC gap would breakdown at $\simeq$ 13 kV RF and a 7 kV DC gap would break down at 6 kV. An RF breakdown is $\simeq$ 85 % of the DC value [31]. Since measured voltage was for the center electrode fed by a resonant RF circuit, the net buncher peak voltage for the beam is twice [34] the calculated value with the case of two-beam gaps driven by the center electrode as seen in Fig. 12.

[1] H. von Jagwitz, U. Hagen, O. Heid, and S. Setzer, in Proc. 2nd Int. Particle Accelerator Conf. (IPAC'11), San Sebastian, Spain, (2011) p. 1725, paper TUPS080.

[2] M. J. de Loos, S. B. van der Geer, Y. M. Saveliev, V. M. Pavlov, A. J.W. Reitsma, S. M. Wiggins, J. Rodier, T. Garvey, and D. A. Jaroszynski, Phys. Rev. Accel. Beams **9**, 084201 (2006).

[3] D. Alt, J. Brandon, D. Leitner, D. Morris, M. Syphers, N. Usher, W. Wittmer, in Proc. Int. Particle Accel. Conf. (IPAC2014), Dresden, Germany (2014), P. 3342, THPME051.

[4] S. B. van der Geer, M. J. de Loos, T. van Oudheusden, W. P. E. M. op t Root, M. J. van der Wiel, and O. J. Luiten, Phys. Rev. Accel. Beams **9**, 044203 (2006).

[5] E. Higgins and G. Paffenroth, IEEE Tran. on Nuclear Sci.,**NS-30**, No. 4, 3484(1983).

[6] P. N. Ostroumov, V. N. Aseev, and B. Mustapha, Phys. Rev. Accel. Beams **7**, 090101 (2004).

[7] T. P. Wangler, RF Linear Accelerator, Wiley-Vch Verlag GmbH and Co. KGaA, 2nd edition, 180-196 (2008).

[8] D. Neuffer, in AIP Conf. Proc. **721** (2004) p. 407. Available at: `http://dx.doi.org/10.`

1063/1.1818445

[9] A. A. Poklonskiya, D. Neuffera, C. J. Johnstonea, M. Berzb, K. Makinob, D. A. Ovsyannikovc, A. D. Ovsyannikovc, Nucl. Instrum. Methods Phys. Res., A **558**, 135, (2006).

[10] Y. K. Batygin, C. Pillai and L. J. Rybarcyk, in Proc. 2011 international Particle Accelerator Conference, San Sebastian, Spain (2011) p. 697.

[11] L. Rybarcyk and S. Kurennoy, in Proc. 2009 Particle Accelerator Conference, New York, (2009) p. 4944.

[12] M. Eshraqi, G. Franchetti, and A. M. Lombardi, Phys. Rev. Accel. Beams **12**, 024201 (2009).

[13] Y. K. Batygin, J. Instrum. (JINST) **15** 07 (2020) P07026.

[14] W. K. H. Panofsky, UCRL-1216 (1951), Maybe available at the University of California library. Also available at https://books.google.co.jp/books?id=VCD5K7Nla3oC&pg=PA1&lpg=PA1&dq=panofsky+#v=onepage&q=panofsky&f=false

[15] L. Smith and R. L. Gluckstern, Rev. of Sci. instrum., **26(2)**, 220 (1955).

[16] G. P. Boicourt, Los Alamos National Laboratory report LA-UR-88-1544 (1988). Available at http://lib-www.lanl.gov/cgi-bin/getfile?00261149.pdf

[17] H. Takeda and J. Billen, PARMILA, Los Alamos Scientific Laboratory,Internal report LA-UR-98-4478, Los Alamos, NM 87545 (2005). Information is available at https://laacg.lanl.gov/laacg/services/download_PMI.phtml

[18] P. W. Lisowski and K. F. Schoenberg, Nucl. Instrum. Methods Phys. Res., A **562**, 910 (2006)

[19] I.N. Draganic, Y.K. Batygin, C.M. Fortgang, R. W. Garnett, J. Gioia, S. S. Kurennoy, R. C. McCrady, J. F. O'Hara, G. Rouleau, and L. Rybarcyk, in Proc. 2013 North America Particle Accelerator Conf.,(2013) p. 667.

[20] T. Wangler and P. W. Lisowski, The LANSCE National User Facility, Los Alamos Science, number 28, (2003) p. 138.

[21] E. J. Peterson, Los Alamos Science, number 30, (2006) p. 112, LANL report number: LA-UR-06-0034. Also available at http://permalink.lanl.gov/object/tr?what=info%3Alanl-repo%2Flareport%2FLA-UR-06-0034

[22] M. S. Moore, Nuclear structure study with neutrons, edited by J Erő' and J. Szűcs, London and New York, (1974), p. 327.

[23] J. D. Cockoroft and E.T.S. Walton, Nature, **129**, 242 (1943).

[24] S. Y. Lee, Accelerator Physics, World Scientific, New Jersey (2004).

[25] K. R. Crandall, TRACE: An interactive Beam-Transport Program, Los Alamos Scientific Laboratory, an Internal report number LA-5332 (1973). A full TECH REPORT entry available at https://www.google.com/url?sa=t&rct=j&q=&esrc=s&source=web&cd=&ved=2ahUKEwijp5j6k9PqAhUKGKwKHYllBpOQFjABegQIAhAB&url=http%3A%2F%2Fdx.doi.org%2F10.2172%2F4434205&usg=AOvVaw3mSoCMZRM9t4lvpXp5KtX2

[26] M. Conte and W. W. Mackay, An Introduction to the Physics of Particle Accelerators, World Scientific (2008).

[27] Y. K. Batygin, I. N. Draganic, C. M. Fortgang, G. Rouleau, in Proc. 2013 international Particle Accelerator Conference, Shanghai, China (2013) p. 1856.

[28] P. K. Roy and Yuri K. Batygin, in Proc. 2016 North America Particle Accel. Conf., Chicago, IL, USA (2016), TUPOA64.

[29] L. Rybarcyk, Improving WNR beam performance, Accelerator Concepts Meeting, Los Alamos National Laboratory, AOT-AE, May 2008. Un-published document. A copy may be available upon request: lrybarcyk@lanl.gov.

[30] P. K. Roy, S. S. Yu, E. Henestroza, A. Anders, F. M. Bieniosek, J. Coleman, S. Eylon, W. G. Greenway, M. Leitner, B. G. Logan, W. L. Waldron, D. R. Welch, C. Thoma, A. B. Sefkow, E. P. Gilson, P. C. Efthimion, and R. C. Davidson, Phys. Rev. Lett. **95**, 234801 (2005).

[31] J. T. M. Lyles, personal communication, 02 Feb (2016), email: jtml@lanl.gov.

[32] C. B. Oler, Trans. of the American Ins. of Electrical Eng., Comu. and Electronics, Part I, 329 (1954).

[33] V.O. Stokes, Radio Transmitters, Van Nostrand Reinhold Inc., U.S, (1970).

[34] L. Rybarcyk, personal communication, 02 Feb 2016, email: lrybarcyk@lanl.gov.

Declaration of Interest Statement

The Primary author (P. K. Roy) has interest in accelerator and beam operation, including particle sources, accelerator sub systems (buncher, chopper, transport elements) , high energy transport lines, circular rings, etc.